

Power density improvement of bi-conductive polymer membrane fuel cells by optimization of its internal resistances

S. Hamel, L.G. Fr  chette

Institut Interdisciplinaire d'Innovation Technologique (3IT), Universit   de Sherbrooke, 3000 Boulevard Universit  , Sherbrooke, J1K 0A5, Qu  bec, Canada

Simon.hamel@usherbrooke.ca

Abstract. This paper reports the development of a new set of equations that defines the internal resistances in bi-conductive membrane (BCM) fuel cells and allows optimization of its critical dimensions and power density. Based on these equations, a design approach is proposed and fabrication steps that limit the power density of the final device are identified. The equations developed in this study can be used for any configuration and shape of holes and current collectors. It demonstrates that by improving fabrication techniques used in a previous study, total internal resistance of the BCM fuel cell could be reduced by 80%, showing that this type of fuel cell could potentially deliver very high power density compared to standard PEMFCs.

1. Introduction

Because of their potentially higher energy density and their instantaneous recharge, polymer electrolyte fuel cells (PEMFCs) are slowly making their way into portable electronic device markets [1]. To become a widespread technology, cost and low energy density issues of PEMFC should however be addressed. To replace the bulky packaging generally used with PEMFCs that significantly reduce their volumetric power density, a new approach to integrate all the necessary components of a fuel cell system on a single layer has been successfully developed in a previous work [2].

Bi-conductive membrane (BCM) fuel cells include on the same layer the current collection, mechanical support and ionic conductive paths and have showed three times better volumetric power density than PEMFC systems with standard packaging (Figure 1). Despite these encouraging results, the areal power density of BCM fuel cells is about 3 times lower than for PEMFCs because of the higher internal resistances generated by this new design. Identifying and quantifying these resistances would allow a better comprehension of BCM fuel cell system and would ease their optimization, thereby increasing the final power density of the device.

In this work, the internal resistances inherent to the BCM fuel cell design are identified and the related analytical equations are developed. This allows the evaluation of the total internal resistance of a BCM fuel cell as a function of its critical dimensions (size of the holes (r_H), spacing (S), radius of patterns (r_P) and membrane thickness (t); Figure 1) and guide the efforts to improve the device.

2. Internal resistances of Bi-conductive membrane (BCM)

To compare easily BCM fuel cells and traditional PEMFCs independently of their area, resistances of fuel cells are evaluated in terms of *area specific resistance*, \tilde{R} ($\Omega \cdot \text{cm}^2$), which when multiplied by the current density per area of electrode J ($\text{A} \cdot \text{cm}^{-2}$) result in the voltage drop in the cell.



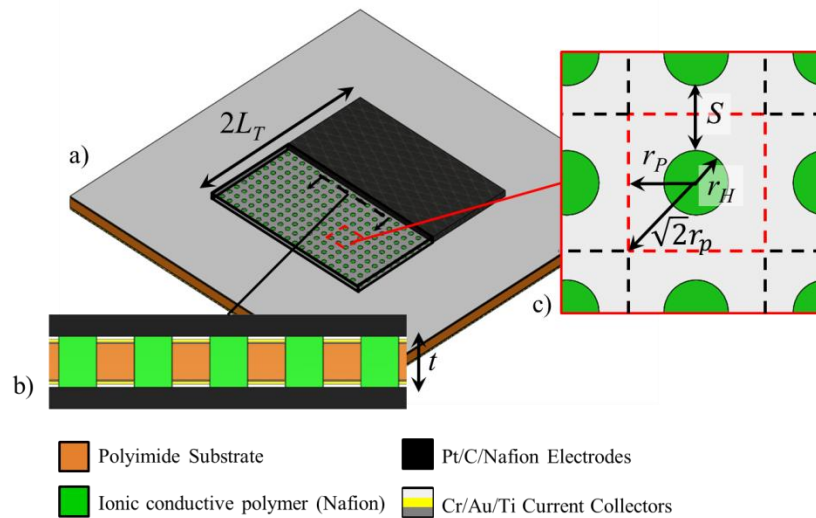


Figure 1 - a) Isometric b) Cross-sectional and c) Close up views of BCPM fuel cell. L_T : Half width of the etched area, t : Thickness of the membrane, r_H : Radius of holes, r_P : Radius of patterns, S : Spacing

In a typical stack configuration, electrons are collected with thick metal grids placed on top of the electrodes while the protons can cross the Nafion membrane which occupies all the volume between the two electrodes. This leads to negligible lateral movements of the electrons and ions in the catalyst layers, hence uniform current generation. In this configuration, the reaction resistance in the catalyst layer (\tilde{R}_{th}) as well as the ionic resistance of the Nafion membrane (\tilde{R}_{IM}) are the main sources of voltage losses in the cell (Figure 2a). In the BCM configuration, a part of the electrons and protons must overcome a lateral electrical (\tilde{R}_{EE}) or ionic (\tilde{R}_{IE}) resistance of catalyst layer, respectively, in addition of \tilde{R}_{th} before the reaction. The effective resistance of the catalyst layer \tilde{R}_E must take into account these lateral and reaction resistances. Also, the ionic resistance of the membrane \tilde{R}_{IM} is increased since an important part of the section between the two catalyst layers is occupied with a non ionic conductive substrate (polyimide). Finally, the lateral displacement of the electrons in the integrated current collectors is also subject to a resistance (\tilde{R}_{EC}) (Figure 2b).

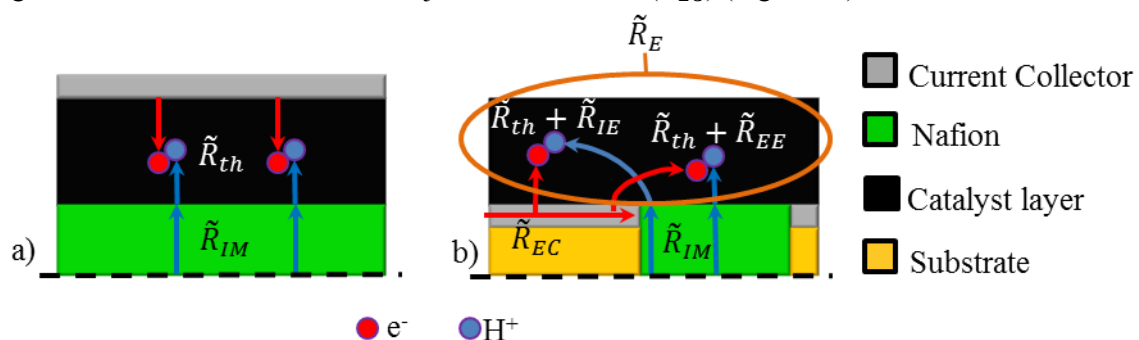


Figure 2 – Area specific resistances in a) half PEMFC with a typical stack configuration and b) half BCM fuel cell.

2.1. Effective resistance of the catalyst layer (\tilde{R}_E)

The electrical and ionic lateral resistances of the catalyst layer (\tilde{R}_{EE} and \tilde{R}_{IE}) generate a non-linear drop of current density away from the junction between the Nafion hole and integrated current collector (ICC) regions. It can be quantified by evaluating the efficiency of the catalyst layer, E_E ,

defined as the ratio between the current that a BCM catalyst layer can provide (I_{P-BCM}) on the current that would have been generated by a standard PEMFC ($I_{P-PEMFC}$) with the same area and \tilde{R}_{th} (Eq. (1)).

$$E_E = \frac{I_{P-BCM}}{I_{P-PEMFC}} \quad (1)$$

For PEMFCs, the generated current can be easily evaluated with Eq. (2) where θ_b is the lost of voltage in the catalyst layer and A its area.

$$I_{P-PEMFC} = \frac{\theta_b}{\tilde{R}_{th}} A \quad (2)$$

For a BCM, because of \tilde{R}_{EE} and \tilde{R}_{IE} , a distributed resistance model must be solved to estimate I_{P-BCM} . To find an analytical expression for I_{P-BCM} , the catalyst layer is modelled as a series of distributed resistances on each side of the junction between the Nafion hole and ICC regions (Figure 3a). Also, as an approximation, the square shape of the ICC surrounding the Nafion hole is first considered as a circle shaped current collector of radius $\sqrt{2}r_p$ (Figure 3b). Produced current is estimated independently in each region of the unit cell and then added up to evaluate total I_{P-BCM} .

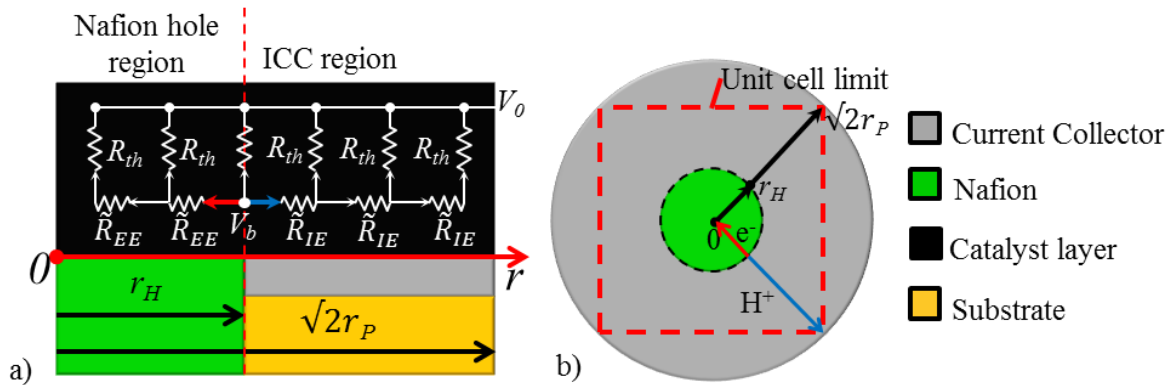


Figure 3 - Top view of BCM (without catalyst layer) illustrating the geometrical limits of the studied zones in the analytical model. b) Distributed resistances model in a cross-sectional view of a BCM.

\tilde{R}_{EE} and \tilde{R}_{IE} vary in function of radial position r because of the radial shape of the unit cell and are proportional to the respective sheet resistance (R_{SE} and R_{SI}) of the catalyst layer. For this work, R_{SE} , have been evaluated to $500\Omega/\text{sq}$ with a 4 probes measurement on commercial catalyst layers (Ion power inc., $0.3 \text{ mg Pt}/\text{cm}^2$). Also, from the work of Boyer et al. [3], the ionic sheet resistance of the electrodes R_{SI} is evaluated to approximatively $10^4\Omega/\text{sq}$.

Current produced in the Nafion hole region (from $r = 0$ to $r = r_H$) is first solved numerically using the distributed resistance model. It was found that the resulting current produced over the Nafion hole region can be approximated with Eq. (3) if r_H is under $500\mu\text{m}$.

$$I_P(0:r_H) = \pi r_H^2 \int_0^{r_H} \frac{V(r)}{\tilde{R}_{EE}(r)} \approx \pi r_H^2 \frac{\theta_b}{\tilde{R}_{th} + \frac{R_{SE}}{9} r_H^2} \quad (3)$$

For the ICC region, by analogy with heat transfer equations for radial fins, an analytical solution can be determined using modified Bessel functions of the first (I) and second (K) kind of zero and first order [4]:

$$I_P(r_H:\sqrt{2}r_p) = \frac{2\pi r_H \theta_b}{R_{SI} \lambda} \cdot \frac{K_1\left(\frac{r_H}{\lambda}\right) I_1\left(\frac{\sqrt{2}r_p}{\lambda}\right) - I_1\left(\frac{r_H}{\lambda}\right) K_1\left(\frac{\sqrt{2}r_p}{\lambda}\right)}{K_0\left(\frac{r_H}{\lambda}\right) I_1\left(\frac{\sqrt{2}r_p}{\lambda}\right) + I_0\left(\frac{r_H}{\lambda}\right) K_1\left(\frac{\sqrt{2}r_p}{\lambda}\right)} \quad (4)$$

where

$$\lambda = \sqrt{\frac{\tilde{R}_{th}}{R_{SI}}} \quad (5)$$

With Eqs. (3) and (4), an analytical solution for the relative efficiency of the catalyst layer, E_E , that includes only the geometrical and resistive terms is defined (Eq. (6)).

$$E_E = \frac{2r_H\lambda}{r_p^2} \cdot \frac{K_1\left(\frac{r_H}{\lambda}\right)I_1\left(\frac{\sqrt{2}r_p}{\lambda}\right) - I_1\left(\frac{r_H}{\lambda}\right)K_1\left(\frac{\sqrt{2}r_p}{\lambda}\right)}{K_0\left(\frac{r_H}{\lambda}\right)I_1\left(\frac{\sqrt{2}r_p}{\lambda}\right) + I_0\left(\frac{r_H}{\lambda}\right)K_1\left(\frac{\sqrt{2}r_p}{\lambda}\right)} + \frac{1}{1 + \frac{R_{SE}}{9\tilde{R}_{th}}r_H^2} \left(\frac{r_H}{\sqrt{2}r_p}\right)^2 \quad (6)$$

The equivalent area specific resistance of one electrode \tilde{R}_E can therefore be evaluated (Eq. (7)):

$$\tilde{R}_E = \frac{\tilde{R}_{th}}{E_E} \quad (7)$$

2.2. Ionic resistance through the membrane (\tilde{R}_{IM})

In a BCM fuel cell, part of the surface is used by the mechanical support thereby reducing the area where the ions can cross from the anode to the cathode and increasing \tilde{R}_{IM} . This resistance is dependant of the ionic resistivity of the Nafion itself ρ_{Nafion} ($\sim 10\Omega \cdot \text{cm}$ [5]), thickness of the membrane, t , and the porosity of the current collector, C (Eq. (8)).

$$\tilde{R}_{IM} = \frac{\rho_{Nafion} \cdot t}{C} \quad (8)$$

Ionic resistance through the BCM is therefore proportional to its thickness and inversely proportional to porosity of the ICC, which is also the area covered with Nafion that can be evaluated for the presented configuration with Eq. (9).

$$C = \frac{\pi}{4} \left(\frac{r_H}{r_p}\right)^2 \quad (9)$$

2.3. Electrical lateral resistance in the ICCs (\tilde{R}_{EC})

When the electrons reach the ICCs, they must be directed to the periphery by the metallic thin film before going in the external circuit. To find \tilde{R}_{EC} , the same model of distributed resistance as for Eq. (3) is used, but a correction factor K_{EC} must be introduced to take into account the large number of etched holes that increase the resistance significantly (Eq. (10)).

$$\tilde{R}_{EC} = K_{EC} \cdot \frac{R_{SC} L_T^2}{\tilde{R}_{th} 9} \quad (10)$$

The value of K_{EC} is evaluated numerically by comparing the loss of voltage of a square porous layer to a plain round one of radius L_T with uniform current. This process has been done for a wide variety of porosity and holes radius. It has been found that for ratio of r_H/L_T under 0.05 (e.g. for a 1 cm^2 fuel cell, $r_{H-Max} = 250\mu\text{m}$), K_{EC} factor is constant for a given porosity. In this case, the correction factor can be expressed solely as a function of porosity C (Eq. (11)):

$$K_{E1} = 35.6C^3 - 26.2C^2 + 10.5C + 0.4 \text{ if } \frac{r_H}{L_T} \leq 0.05 \quad (11)$$

2.4. Performance index and fabrication limitations

To facilitate design of BCM fuel cells, the total resistance of a standard fuel cell can be compared to the total resistance of the new configuration of the same dimension resulting in its performance index, P_I (Eq. (12)).

$$P_I = \frac{\tilde{R}_{IM-PEMFC} + 2\tilde{R}_{th}}{2\tilde{R}_E + 2\tilde{R}_{EC} + \tilde{R}_{IM}} \quad (12)$$

This index gives a relative performance of the selected dimensions and allows quick comparison of a wide range of configurations. In this work, a commercial Ion power Inc. fuel cell with a $50\mu\text{m}$ thick

NR-212 Nafion membrane and catalyst loading of 0.3 mg Pt/cm^2 is used as a references in the evaluation of P_I . By extracting data from its polarization curves performed at 40°C and saturated flows conditions, it was established that its total resistance was equal to $0.3 \Omega \cdot \text{cm}^2$.

P_I depends on the critical dimensions r_H , S and t which are limited by available technologies and materials, and greatly influence optimization of the BCM. For example, in the preceding work of Hamel et al. [2], r_H was restricted to a minimum of $10 \mu\text{m}$ due to the precision of the chosen etching technique and S to $50 \mu\text{m}$ to avoid delamination of the ICCs during the fabrication process. Furthermore, a minimal ratio of 0.5 between r_H and t was needed to ensure a complete filling of the holes.

With these fabrications limitations, the optimal P_I for a variety of critical dimensions can be estimated. Figure 4 illustrates the variation of P_I as a function of r_H and C for a Kapton sheet of $50.8 \mu\text{m}$ or $25.4 \mu\text{m}$ thick. The red dotted lines represent the superior limit of P_I for a given S and the dark regions are the possible critical dimensions depending on fabrication limitations. With fabrication limitations stated in [2], the possible combinations are limited to porosities under 0.2 and the best theoretical P_I is 0.4 for $r_H = 25 \mu\text{m}$ and $S = 50 \mu\text{m}$. Incidentally, these dimensions have been selected in [2], with an experimental P_I of 0.31, relatively close to the predicted value.

Figure 4 also shows achievable P_I if S can be reduced to $25 \mu\text{m}$ and $(r_H/t)_{\text{max}}$ increased to 1. These improvement could increase the maximum value of P_I from 0.4 to 0.65 while keeping $t = 50.8 \mu\text{m}$, but could be increased to 0.72 is using a thinner Kapton membrane ($25.4 \mu\text{m}$). It demonstrates that achievable improvement in fabrication techniques could lower the total internal resistance of BCM fuel cell by 80%.

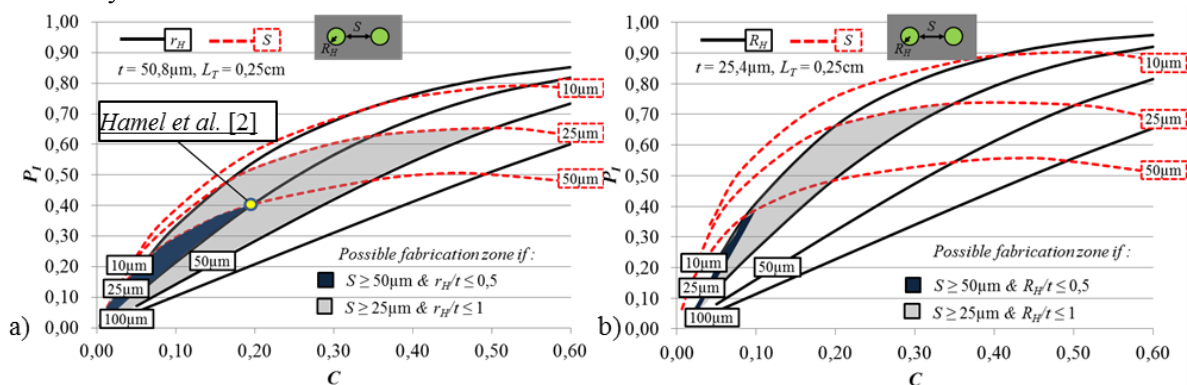


Figure 4 - Performance index of the BCM fuel cell design in function of critical dimensions and fabrication limitations for a) $t = 50.8 \mu\text{m}$, b) $t = 25.4 \mu\text{m}$, and $L_T = 0.25 \text{ cm}$.

3. Conclusion

The set of equations developed in this paper give simple guidelines to design a BCM fuel cell and limit its internal resistances. It has been shown that fabrication limitations greatly affect the choice of dimensions and should be taken into account at the beginning of the design process.

Simple improvements to the fabrication techniques presented in a preceding work [2] could lead to an areal current density of the BCM of 80%, increasing even more the dominance of this type of fuel cell when it comes to volumetric power density.

References

- [1] S.-G. Kim and S.-J. Lee, "A review on experimental evaluation of water management in a polymer electrolyte fuel cell using X-ray imaging technique," *J. Power Sources*, vol. 230, pp. 101–108, May 2013.
- [2] S. Hamel, T. Tsukamoto, S. Tanaka, and L. G. Fr  chette, "Microfabrication of a Polymer Based Bi-Conductive Membrane for a Polymer Electrolyte Membrane Fuel Cell," *J. Phys. Conf. Ser.*, vol. 476, p. 012109, Dec. 2013.